Model Wind Optimization with Satellite Wind Observations for Operational Sea Level Prediction

Francesco De Biasio[1,2], **Stefano Zecchetto**[3]

1. National Research Council - Institute of Polar Sciences. Via Torino 155, Venezia, Italy
2. Ca' Foscari University of Venice. Via Torino 155, Venezia, Italy
3. National Research Council - Institute of Polar Sciences. Corso Stati Uniti 4, Padova, Italy

Abstract

Sea surface wind forecasts in the Adriatic Sea often suffer for unadequate modelling, especially for the wind speed. This has detrimental effects on the accuracy of sea level and storm surge predictions. We present a numerical method to reduce the bias between the sea surface wind observed by the scatterometers and that supplied by the European Centre for Medium-Range Weather Forecasts (ECMWF) global atmospheric model, for storm surge forecasting applications. The method, called "wind bias mitigation", relies on scatterometer observations to determine a multiplicative factor Δws which modulates the standard model wind in order to decrease the bias between scatterometer and model. We compare four different mathematical approaches to this method, for a total of eight different formulations of the multiplicative factor Δws. Four datasets are used for the assessment of the eight different bias mitigation methods: a collection of 29 Storm Surge Events (SEVs) cases in the years 2004-2014, a collection of 48 SEVs in the years 2013-2016, a collection of 364 cases of random sea level conditions in the same period, and a collection of the seven SEVs in 2012-2016 that were worst predicted by the *Centro Previsioni e Segnalazioni Maree, Comune di Venezia* (Tide Forecast and Early Warning Centre of the Venice Municipality - CPSM). The statistical analysis shows that the bias mitigation procedures supplies a mean wind speed more accurate than the standard forecast, when compared with scatterometer observations, in more than 70% of the analyzed cases.

INTRODUCTION

Storm surges are intense increases of sea level, caused by severe meteorological conditions. Several coastal regions of the northern Adriatic Sea are threatened by inundations due to storm surges, caused by the Sirocco wind, blowing from south-east along the Adriatic Sea longitudinal axis, assisted by the Bora wind which often forms after an intense Sirocco event, and blows from north-east. The most popular example is the city of Venice. In the last 150 years an evident positive trend has been registered in Venice for both the yearly number of high water events and the mean sea level height, as shown in Fig. 1 (Courtesy of *Centro Previsioni e Segnalazioni Maree, Comune di Venezia* (Tide Forecast and Early Warning Centre of the Venice Municipality - CPSM) `http://www.comune.venezia.it/it/content/variazioni-livello-medio-mare`). The trend is likely to persist in the next decades (Church et al., 2013), and even if the mobile barrier system MOSE has been realized and has started to protect Venice and its lagoon from floodings since late 2020 (`http://www.mosevenezia.eu/`), nonetheless it is necessary to predict and monitor the storm surges approaching the Gulf of Venice, to prevent risks and damages, and to manage the closing and opening of the mobile barriers to minimize the negative impact on the economic, health and emergency sectors and on the transport of people and goods.

Storm surge models (SSMs) are routinely used to forecast the sea level in the Gulf of Venice and inside the Venice Lagoon in order to prevent risks and to ensure the continuity of all the public services. The SSMs rely on numerical weather prediction (NWP) model fields of wind and pressure as forcing input. The initial conditions of the surge at the beginning of the forecast simulation, namely the sea surface vertical displacement and the water transport zonal and meridional components, are also needed in order to perform realistic simulations of the surge. The quality of the NWP wind forcing has a direct impact on the accuracy of the modeled surge, as forcing input errors are propagated by the SSM, and amplified by the inherent approximations in the SSM formulation and in the hydrodynamic initial and boundary conditions. It is thus essential to supply to the SSMs forcing inputs as close as possible to the real meteorological situation. As diffuse and accurate observations of the sea surface wind are

Preprints (www.preprints.org) | NOT PEER-REVIEWED | Posted: 28 December 2022 doi:10.20944/preprints202212.0531.v1

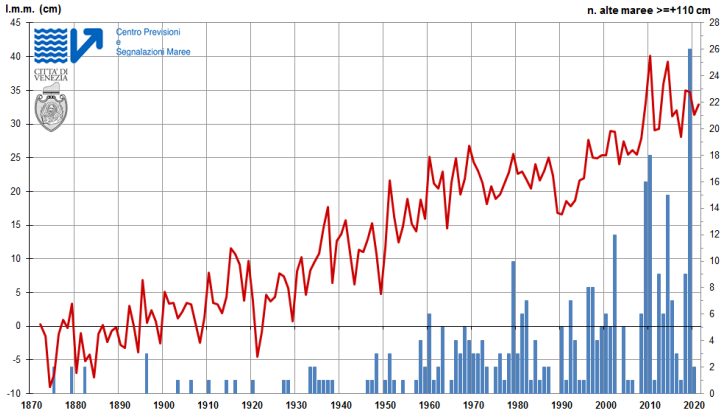

Figure 1: **The mean sea level and the annual number of high tides $\geq$ 110 cm registered in Venice in the period 1872-2021. Note: MOSE system has been operational since December 2020 (Courtesy of Centro Previsioni e Segnalazioni Maree, Comune di Venezia).**

possible today with satellite-borne scatterometers, it is worthwhile to assess a methodology able to exploit satellite wind observations for storm surge modeling purposes.

The Data User Element (DUE) program of the European Space Agency (ESA) funded the project *eSurge-Venice*, aimed to demonstrate the improvement of the storm surge forecasting through the use of earth observation data, with focus on the Gulf of Venice. The project ended in 2015. An important achievement of the project was the development of the wind bias mitigation procedure (WBM), which uses scatterometer observations to adjust the model forecast wind fields for use as forcing input in a storm surge model. The WBM procedure has proved to be able to reduce the model-scatterometer wind bias and improve the performance of a storm surge model (De Biasio et al., 2016, Bajo et al., 2017, De Biasio et al., 2017).

As an isolated topic, distinguished from the specific context of storm surge forecasting, the WBM procedure was first introduced by Zecchetto et al. (2015), who assessed the performance of WBM in a dataset consisting of thirty-three cases of high water in Venice in the period 2004-2014. These cases were selected as occurring at the same time of significant storm surges observed in the Gulf of Venice. The assessment regarded the improvements brought by scatterometer observations through the WBM procedure to the sea surface wind forecasts provided by the European Centre for Medium-Range Weather Forecasts (ECMWF) global atmospheric model.

In these experiments, the WBM methodology relied on a simple yet effective algorithm to determine the bias, and remodulate the model wind field. Having the WBM methodology reached a decent level of maturity, we now want to investigate a number of different datasets, using different mathematical approaches to the WBM algorithm for the wind speed, in order to statistically determine the more suitable one.

In the SSMfollowing sections, firstly we describe the main differences between model and scatterometer sea-surface wind fields as seen in the Adriatic Sea. Then, the satellite and model data used in this study are presented, followed by the description of the WBM procedure. A characterization of the different mathematical approaches to the WBM algorithm is given before the section presenting the statistical results. The last section is dedicated to the conclusions.

DIFFERENCES BETWEEN MODEL AND SCATTEROMETER WINDS IN THE ADRIATIC SEA

The Adriatic Sea is a semi-enclosed basin of elongated shape in the direction SE-NW and surrounded by mountain chains. Its open mouth in the south-eastern side is connected with the Ionian Sea and the Mediterranean basin (see 2): these characteristics favour the occurrence of storm surges in the northern (closed) end, generated by south-eastern winds, in particular during autumn and winter and with higher elevations than in the rest of the Mediterranean Sea. Often after a surge driven by Sirocco, the mesoscale atmospheric circulation forces the set up of Bora wind from north-east, which pushes the water already collected by Sirocco in the Gulf of Venice, against the three mouths of the Venice Lagoon, contrasting the flow of the high water from inside the lagoon through the three inlets.

The meteorological condition responsible for the occurrence of storm surges in the Gulf of Venice is a deep low-pressure system situated west of the Adriatic Sea, usually over the Thyrrenian Sea. It causes the sirocco –

Preprints (www.preprints.org) | NOT PEER-REVIEWED | Posted: 28 December 2022 doi:10.20944/preprints202212.0531.v1

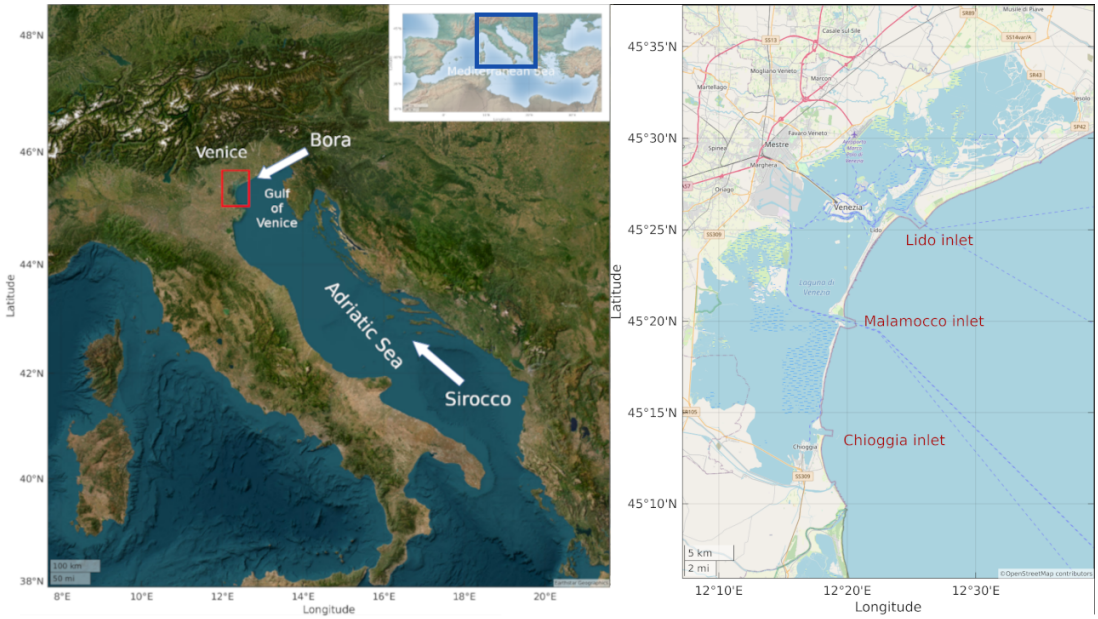

Figure 2: **Left: the Adriatic Sea bathymetry and its geographical orientation. Bora blows from North-East, Sirocco from South-East. In the northern part of the Adriatic Sea the Gulf of Venice gathers the water pushed by storms from SE and NE, triggering the high water at the coast and inside the Venice Lagoon. The inset map in the upper right corner shows the position of the Adriatic Sea inside the Mediterranean area. The red circle marks the position of Venice and its lagoon. The red box, marking the position of the Venice Lagoon in the Adriatic Sea, is enlarged to the right of the Figure. Right: The Venice Lagoon with its three inlets, facing the Gulf of Venice.**

a wet and warm wind from south-east – to blow along the Adriatic major axis (Lionello et al., 2012). Often in the southern and central parts of the basin blows the sirocco, while in the northern basin the wind comes from north-east (bora): this configuration often happens when the cyclonic circulation moves from the ThyrreniaSSMn to the Adriatic side of the Italian peninsula, forming an arch over the Adriatic basin.

When the focus comes on storm surge model forecasts, it is thus desirable to have accurate wind field forecasts available. A relatively simple way to estimate the accuracy of NWP model sea surface winds is to compare them with scatterometer observations.

Previous works comparing scatterometer observations and NWP model forecasts were based on the analysis of a high number of observed and simulated collocated data. Accadia et al. (2007) compared QuikSCAT L2B 25 km observations and wind field forecasts produced by the Quadrics Bologna Limited-Area Model (QBOLAM) over the Mediterranean Sea. They found areas of lower than average forecast skill, and identified these areas as being semi-enclosed basins surrounded by rough orography. Kara et al. (2009) compared, on a monthly basis, the QuikSCAT 25 km data with "analysis quality" NWP winds (A. Wallcraft, personal communication, 2014) coming from the NOGAPS dataset at 0.5° of resolution, in the Mediterranean Sea.

Zecchetto et al. (2015), proposed a new methodology for exploiting satellite-borne scatterometer wind observations to reduce the bias of numerical model prediction wind fields with respect to satellite-detected winds.

De Biasio et al. (2016, 2017), Bajo et al. (2017) toke advantage of the methodology described in Zecchetto et al. (2015), adapting a combined strategy, based on satellite scatterometry and satellite altimetry, in order to improve the prediction skills of a hydrodynamic model used for strom surge forecast in the Adriatic Sea and Venice, with positive results. In their study, the surface wind field was provided by the ECMWF numerical atmospheric model, scatterometer winds were derived from the SeaWinds scatterometer mounted on the American NASA QuikSCAT satellite, and from the ASCAT instruments onboard the European MetOP satellites. Altimetry data were provided by the Center for Topographic Studies of the Ocean and Hydrosphere (CTOH), and assimilated in the numerical hydrodynamic model. Separate reanalysis for several historical Storm Surge Events (SEVs) in the Adriatic Sea were conducted using both scatterometer winds and altimetry sea level heights, only one of the two, and withous Earth Observation (EO) data (control runs). In almost all the cases the reanalysis experiments with EO data performed better than the control runs.

Byrne et al. (2017) applied a technique similar to that described in Zecchetto et al. (2015), to improve the forecast of storm surges, and tested it in three hurricane events landfalling at the US coast. They used the analysis

Preprints (www.preprints.org) | NOT PEER-REVIEWED | Posted: 28 December 2022 doi:10.20944/preprints202212.0531.v1

wind fields produced by the Multi-Platform Tropical Cyclone Surface Wind Analysis (MTCSWA), developed by the National Hurricane Center (Florida, US), as forcing into a storm surge hydrodynamic model. The forcing winds were produced by multiplying the parametric wind field zonal and meridional components by a factor (innovation factor, IF) depending on the parametric and the analysis wind fields at the previous time step. Differently from the studies of the previous authors, considering only wind speed, the formulation proposed in these three experiments acts on the zonal and meridional components independently. Apart from this aspect, the mathematical algorithm is similar.

In general, coastal areas surrounded by significant orography, in the cited bibliography were found to negatively affect the atmospheric modelling performance. The approachces proposed by Zecchetto et al. (2015) and Byrne et al. (2017), are similar and can be implemented easily and quickly, but little attention has been given, in our knowledge, to the analysis of the proposed algorithm. In this study we briefly analyze such algorithm, and also propose possible alternatives to it, for the modification of the forcing wind using EO data. We assess the performances of the original algorithm and of their alternatives applying them to four datasets which can be seen to form the general phenomenology of the storm surge in the northern Adriatic Sea.

WIND DATA

The numerical weather prediction model data

As forcing, in the comparison we used the analysis and forecast wind fields of the global deterministic model operating at different resolutions (from 40 km to 16 km of equivalent grid, depending on the period), of the ECMWF, provided at synoptic hours (at 00, 06, 12, 18 UTC analysis; three-hourly forecast) and interpolated on a 0.125° regular grid. The wind components are given at 10 m of height from the sea surface and at real air-sea stability conditions. For forecast winds we have kept the forecast valid time within twenty-four hours of the base time (midnight).

The scatterometer wind data

Satellite-borne scatterometers remotely sense the roughness of the sea surface, which is in equilibrium with the wind, and reveal the wind speed and direction by inversion of the radar backscatter values. The scatterometer data used in this work is the NASA QuikSCAT version 3 L2B Ocean Wind Vector (OWV) 12.5 km (1999-2009) (JPL, 2013b), the EUMETSAT ASCAT-A L2 OWV 12.5 km (2009-2015), ASCAT-A L2 Coastal OWV 12.5 km (2010-present), ASCAT-B L2 Coastal OWV 12.5 km (2012-present) (OSISAF, 2012) and Oceansat-2 L2B OWV 12.5 km (2010-2014) (JPL, 2013a). Scatterometer winds are given in ”equivalent neutral” atmospheric conditions, contrary to the numeric prediction data. As real meteorological conditions have in general different conditions of stratification at the air-sea interface, which influence the energy and momentum exchange between the two media differently, the scatterometer neutral winds have been corrected for the effects of the atmospheric stability, using a boundary layer model W.T. Liu and K.B. Katsaros and J.A. Businger (1979) as described in Zecchetto et al. (2013). The bulk quantity used for the correction are the air and dew temperature fields at 2 m height on the mean sea level of the ECMWF model, and the Operational Sea Surface Temperature and Sea Ice Analysis (OSTIA, Stark et al. (2007)) maps provided by the Physical Oceanography Distributed Active Archive Center (PO.DAAC, Jet Propulsion Laboratory (JPL), Pasadena, California). The scatterometer data have been interpolated on the same 0.125° regular grid used for ECMWF data with a Laplacian method which does not influence the statistics of the wind speed and direction (Accadia et al., 2007).

THE WIND BIAS MITIGATION PROCEDURE

Our study focuses on the comparison of ECMWF model wind analysis and forecast data with scatterometer winds, keeping the latter as the term of reference. We also investigate on the possible use of the scatterometer winds as a tool to improve the accuracy of the predicted wind fields, as our objective are operational SSM applications in the Gulf of Venice. As such, we concentrate the comparison geographically on the Adriatic Sea. Here, the ECMWF global atmospheric model supply very high-quality forecast and analysis of the sea surface wind fields, which however are in general underestimated. Zecchetto, S. and Accadia, C. (2014) have found that scatterometer-model wind bias in this area are greater close to coast, and the differences between models and satellite winds are variable in space and time. The scatterometer-model bias can be used to adapt the NWP wind fields to observations wherever the bias is relevant.

Preprints (www.preprints.org) | NOT PEER-REVIEWED | Posted: 28 December 2022 doi:10.20944/preprints202212.0531.v1

Preliminary investigations of differences and similarities between scatterometer and model winds have been carried out by means of the relative wind speed bias $\delta w^N(i,j,t)$ (Accadia et al., 2007, Zecchetto et al., 2013, Zecchetto, S. and Accadia, C., 2014), defined as:

$$\delta w^N(i,j,t) = \frac{w^s(i,j,t) - w^m(i,j,t)}{w^s(i,j,t)} \tag{1}$$

where $w(i,j,t)$ is the wind speed at time t and location (i,j) of the 0.125° x 0.125° regular grid covering the area. The superscripts "s" and "m" refer to scatterometer and model respectively. Statistically reliable quantities for the relative wind speed bias are derived averaging locally Δw^N over a given period:

$$\Delta w^N(i,j) = \left\langle \frac{w^s(i,j) - w^m(i,j)}{w^s(i,j)} \right\rangle = \frac{1}{N}\sum_{k=1}^{N} \frac{w_k^s(i,j) - w_k^m(i,j)}{w_k^s(i,j)} \tag{2}$$

where the temporal average is represented as the sum over a number N of time instants $t_1, t_2, ..., t_k, ..., t_N$, and the dependence from time has been substituted by the discrete index "k".

The representation of the statistics of the bias averaged over a period of almost two years (January 2008-November 2009) is reported in Fig. 3: the relative bias between the two datasets is always positive (ECMWF underestimates winds with respect to scatterometer), reaching the 25% along coasts.

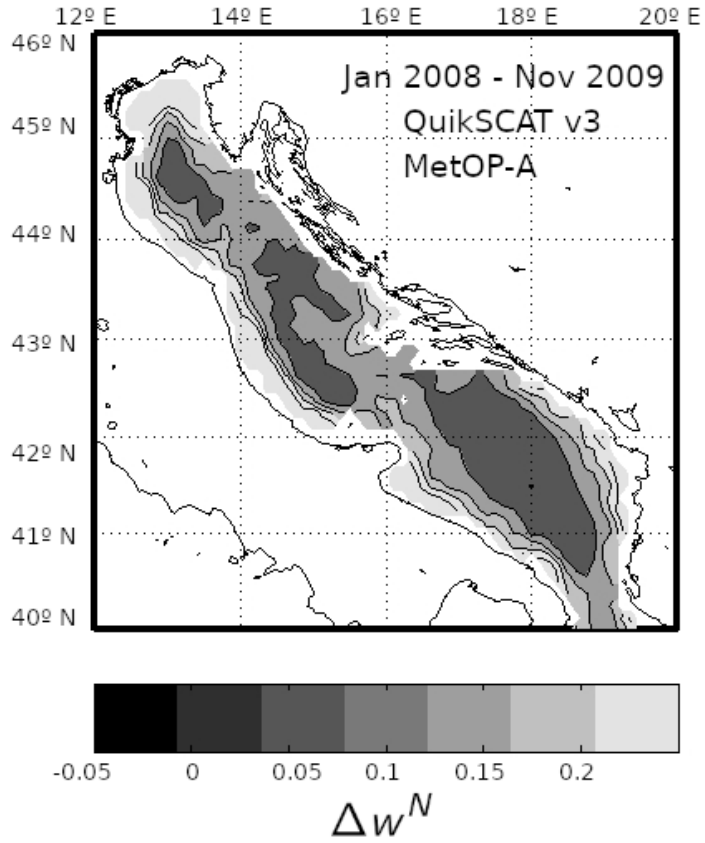

Figure 3: **Scatterometer-ECMWF wind speed relative bias for the period January 2008 to November 2009. Scatterometer observations are from QuikSCAT and MetOP-A missions.**

The average number of scatterometer passes over the Adriatic Sea is around 3-4 times a day, with maxima during limited periods of simultaneous operations of QuikSCAT/MetOP-A and Oceansat-2/MetOP-A and -B (4-6 passes a day). With such low number of collocated scatterometer-model data at each grid point, it is necessary collect and average scatterometer observations during a period of some days in order to obtain statistically reliable quantities. However, enlarging arbitrarily the averaging window would turn to a loss in correlation between observations pertaining to different meteorological patterns, thus reducing their statistical significance. For the present application the optimal size of the averaging period resulted to be three days (Zecchetto et al., 2015).

Preprints (www.preprints.org) | NOT PEER-REVIEWED | Posted: 28 December 2022 doi:10.20944/preprints202212.0531.v1

An intuitive way to perform a tuning of the model wind speed is using the relative wind speed bias calculated in eq. 2. The wind tuning process, also called wind bias mitigation, has been first proposed and investigated in Zecchetto et al. (2015). In that study the relative wind speed bias $\Delta w^N(i,j)$ was used as a counteracting term, in order to *nudge* the model values toward the scatterometer retrievals, i.e.

$$w'^m(i,j) = w^m(i,j)\left(1 + \Delta w^N(i,j)\right) \tag{3}$$

where the prime symbol marks the bias-mitigated forecast wind speeds, and the quantity $\left(1 + \Delta w^N\right)$ is called bias mitigation factor (BMF). The relative wind speed bias, calculated over the running averaging window of three days, is used to modify the NWP wind fields of the first day following the averaging window. The process is repeated for every day of the period subject to mitigation, so that a time series of daily wind bias mitigation factor maps, covering that period, is generated. In our study, the surge events (SEVs, or "cases") are defined as a sequence of three days: for each of these three days (say A, B and C), a single bias-mitigation map is formed, considering the relative wind speed bias calculated with the collocated model *analysis* and scatterometer wind speed values of the previous three days, as described by eq. 2. Then, the bias-mitigation map is used to mitigate the bias of the model *forecast* wind speed of day A, B and C separately, as prescribed by eq. 3. Finally, the three days A, B and C are considered together, and a statistical analysis of the bias-mitigated model forecast, the original model forecast and the scatterometer observations is performed. To assess the performance of the WBM procedure, mitigated and non-mitigated forecast wind speed values are compared against the scatterometer-collocated ones, which in our analysis represent the ground thruth. It is important to underline that in our study we compare (modified) model wind fields against scatterometer wind fields, and the statistical analysis is based exclusively on such comparison: we do not consider surge levels of any kind in the following results.

The statistical analysis has been conducted on four different datasets:

- **DATASET D1**: 29 SEVs (observed surge >40 cm) during the years 2004–2014. Dataset D1 is the same used by Zecchetto et al. (2015), for which the overlapping SEVs have been removed. This dataset has been considered here as it was first used by Zecchetto et al. (2015), and thus represents a natural test bed for the alternative mathematical approaches that we will introduce later;
- **DATASET D2**: 48 SEVs (observed surge >40 cm) during the years 2013–2016, among the years with the highest number of high waters in Venice. It is the natural continuation of dataset D1 over the following years. Note that, while in 2004–2014 we count 29 SEVs, i.e. 2.6 SEV per year, in 2013–2016 this figure has rise to 12.0 SEV per year;
- **DATASET D3**: 364 cases during the years 2013–2016. Dataset D3 is made of random surge level cases. It has been formed considering the years 2013–2016, as for dataset D2, but picking one case every five days, starting from January, 7th 2013. In these cases the wind is random and not related to storm surges. It is thus a good candidate to test the effectiveness of the WBM procedure in meteorological conditions not directly related to storm surges;
- **DATASET D4**: 7 SEVs in 2012–2016. These were the seven SEVs worst predicted by CPSM (A. Tosoni, 2017 - personal communication).

ORIGINAL AND ALTERNATIVE MATHEMATICAL APPROACHES FOR THE CALCULATION OF THE BIAS MITIGATION FACTOR

The original formulation of the model wind speed correction factor $(1 + \Delta w^N)$ in eq. 3 Zecchetto et al. (2015), hencefort indicated as "Original Formulation" (**OF**)), was developed heuristically. As a consequence, its definition is weak, as it could occasionally take also negative values. Omitting the spatial indexes (i,j) in the following discussion, we have:

$$1 + \Delta w^N_{OF} = 1 + \left\langle \frac{w^s - w^m}{w^s} \right\rangle = 1 + \frac{1}{N}\sum_{k=1}^{N} \frac{w^s_k - w^m_k}{w^s_k} = 2 - \frac{1}{N}\sum_{k=1}^{N} \frac{w^m_k}{w^s_k} \tag{4}$$

When $\sum_{k=1}^{N} \frac{ws(t_k)_{model}}{ws(t_k)_{scatt}} > 2N$ the factor $(1 + \Delta w^N)$ is oddly defined, tacking negative values and giving origin to negative wind speeds (see eq. 3). Infact, for a small number of collocated model and scatterometer observations at the same location (i,j), and/or for small wind speeds and/or particularly unfortunate predictions, or when the meteorological conditions change drastically during the same SEV in a short period of time, it is not unlikely that many or all of the terms in the sum $\sum_{k=1}^{N} \frac{ws(t_k)_{model}}{ws(t_k)_{scatt}}$ are grreater than two, so that they add-up

Preprints (www.preprints.org) | NOT PEER-REVIEWED | Posted: 28 December 2022 doi:10.20944/preprints202212.0531.v1

to something $> 2N$. A partial solution to this problem is to perform the mitigation process based on thresholds which can be adapted easily in order to prevent such situation. Nonetheless, as we will see, eq. 3 works rather well, putting a lower threshold of 0 to the values in the bias-mitigation maps.

In our opinion, however, it is more desirable to formulate alternative and well-defined algorithms, in order to obtain consistently defined mitigation factors (MF). This brought us to consider several approaches to define a consistent WBM algorithm. They are:

- **Alternative formulations (AF1 and AF2)**: they are based on the definition of the **OF**, but the denominator is substituted with a more suitable quantity, which prevents the bad behaviour of **OF**. The quantity in the denominator of **AF1** is the model wind speed (eq. 5); that in **AF2** is is the mean values of the model and the scatterometer wind speed (eq. 6);

$$1 + \Delta w^N_{AF1} = 1 + \left\langle \frac{w^s - w^m}{w^m} \right\rangle \tag{5}$$

$$1 + \Delta w^N_{AF2} = 1 + \left\langle \frac{w^s - w^m}{\frac{1}{2}(w^{sc} + w^m)} \right\rangle \tag{6}$$

  In **AF1** the increment in wind speed is relative to the model wind instead to the scatterometer wind. This choice is better defined that **OF** as $1 + \Delta w^N_{AF1} = \frac{1}{N}\sum_{k=1}^{N} \frac{w^s_k}{ws^m_k}$, i.e. it is positive defined, unless some of the model wind speed are equal to zero.
  In **AF2** the increment in wind speed is relative to the mean value of model and scatterometer wind speed at each step t_k. As one can easily see, in such case the mitigation factor $1 + \Delta w^N_{AF1}$ is equal to $\frac{2}{N}\sum_{k=1}^{N} \frac{w^s_k}{\overline{w_k}}$, where $\overline{w_k} = \frac{w^s_k + w^m_k}{2}$, and results always ≥ 0 and well-defined, unless at least one of the $\overline{w_k}$ is zero;

- **Analytical solution (AS)**: It is determined from the definition of bias-mitigated model wind (eq. 3):

$$w'^m_k = w^m_k \left(1 + \Delta w^N\right),$$

  and imposing that the relative wind speed bias between the bias-mitigated model wind speeds and the scatterometer wind speed is zero (primed quantities are the mitigated-ones):

$$\left\langle \frac{w^s - w'^m}{w^s} \right\rangle = 1 - \left\langle \frac{w'^m}{w^s} \right\rangle = 0. \tag{7}$$

  Substituting the expression of eq. 3 for w'^m in eq. 7, we have:

$$\sum_{k=1}^{N} \frac{w^s_k - \left(1 + \Delta w^N\right) w^m_k}{w^s_k} = N - \left(1 + \Delta w^N\right) \sum_{k=1}^{N} \frac{w^m_k}{w^s_k} = 0 \tag{8}$$

  and thus:

$$1 + \Delta w^N_{AS} = \left[\frac{1}{N} \sum_{k=1}^{N} \frac{w^m_k}{w^s_k} \right]^{-1} \tag{9}$$

- **Least square regression approach:** A vast class of optimal solutions to the bias-mitigation procedure comes from the least square regression approach (LSR). In the following, we consider two classes of solution, the first is said "linear", the second "relative", obtained by minimizing specific functions of the residuals, which depend from the wind speed of scatterometer and model, and a parameter α:

$$\begin{cases} \delta_\alpha & = & f(w^s_k, w^m_k, \alpha) \\ \frac{\partial \delta_\alpha}{\partial \alpha} & = & 0 \end{cases}$$

  – **Linear least square regression approach (LLSR and LLSR$_E$)**: linear LSR is used to minimize the classical sum of the squared residuals of the scatterometer minus model wind speeds, with respect to the parameter α, which corresponds to the Δw^N to be determined.

Preprints (www.preprints.org) | NOT PEER-REVIEWED | Posted: 28 December 2022 doi:10.20944/preprints202212.0531.v1

The first approach considered in this study is the simplest: the function to be minimized is the squared sum of the residuals formed by the scatterometer and the bias-mitigated model wind speeds. The parameter α is hidden in the definition of the latter:

$$\delta_\alpha = \sum_{k=1}^{N} [w_k^s - w_k'^m]^2 = \sum_{k=1}^{N} [w_k^s - (1+\alpha) w_k^m]^2$$

the solution in this case is given by:

$$1 + \Delta w_{LLSR}^N = \frac{\sum_{k=1}^N w_k^m w_k^s}{\sum_{k=1}^N (w_k^m)^2}$$

The second of the linear LSR approaches (LLSR$_E$), minimizes the sum of the squared differences of the *squared scatterometer and model wind speeds*. The latter formulation of the LLSR approach was suggested in order to take into consideration the quadratic dependence of the sea surface wind stress on the wind speed (Pugh, 1987), as well as the dependence of the surge level on the square of the wind speed in theoretical (Pugh, 1987) and empirical (Silvester, 1971) models:

$$\delta_\alpha = \sum_{k=1}^{N} \left[(w_k^s)^2 - (w_k'^m)^2\right]^2 = \sum_{k=1}^{N} \left[(w_k^s)^2 - (1+\alpha)^2 (w_k^m)^2\right]^2$$

and the solution is:

$$1 + \Delta w_{LLSR_E}^N = \left[\frac{\sum_{k=1}^N (w_k^m)^2 (w_k^s)^2}{\sum_{k=1}^N (w_k^m)^4}\right]^{\frac{1}{2}}$$

– **Relative least square regression approach (RLSR and RLSR$_E$)**: relative regression (Tofallis, 2008) has been suggested in those cases where relative variations are more significant than absolute variations, and thus perfectly fits the problem we are facing here. Even in the Relative LSR we adopted two minimization approaches: the first (RLSR) minimizes the sum of the squared differences of the scatterometer and model wind speed, weighted by the inverse of the scatterometer wind speed:

$$\delta_\alpha = \sum_{k=1}^{N} \left[\frac{w_k^s - w_k'^m}{w_k^s}\right]^2 = \sum_{k=1}^{N} \left[\frac{w_k^s - (1+\alpha) w_k^m}{w_k^s}\right]^2$$

with solution:

$$1 + \Delta w_{RLSR}^N = \frac{\sum_{k=1}^N \frac{w_k^m}{w_k^s}}{\sum_{k=1}^N \left(\frac{w_k^m}{w_k^s}\right)^2}$$

The second (RLSR$_E$) minimizes the sum of the squared differences of the scatterometer and model *squared* wind speeds, with the same weight as before.

$$\delta_\alpha = \sum_{k=1}^{N} \left[\frac{(w_k^s)^2 - (w_k'^m)^2}{w_k^s}\right]^2 = \sum_{k=1}^{N} \left[\frac{(w_k^s)^2 - ((1+\alpha) w_k^m)^2}{w_k^s}\right]^2$$

with solution:

$$1 + \Delta w_{RLSR_E}^N = \left[\frac{\sum_{k=1}^N (w_k^m)^2}{\sum_{k=1}^N \frac{(w_k^m)^4}{(w_k^s)^2}}\right]^{\frac{1}{2}}$$

As in some cases the algorithms of the WBM give wind speeds beyond the physical limits found in the Mediterranean Sea, we have thresholded the mitigated winds to 33 ms^{-1}.

Preprints (www.preprints.org) | NOT PEER-REVIEWED | Posted: 28 December 2022 doi:10.20944/preprints202212.0531.v1

STATISTICAL RESULTS

The probability distribution of the MFs $(1 + \Delta w^N)$ for the D3 dataset, as an exemple, is depicted in Fig. 4: on the left panel the distributions of the MF for the LSR methods are reported, while in the right panel are shown the MFs of the other four methods (OF, AF1, AF2 and AS), all in a *semilog-y* scale. The anomalous behaviour of the OF MF distrbution is evidenced by the plots of the right panel of the figure: it allows negative values, and exhibits a characteristic profile, different from the other MFs, falling down to zero at (near) 2: this value is derived directly from eq. 4, when all the w_k^m are equal to zero. All the other MF distributions do not take negative values and extends towards much higher values on the positive side of the *x-axis*. The statistical summary reported in table 1 shows that the distribution of the OF MF is the only one whith negative skewness. It is also the one which mostly follows the normal distribution (skewness -0.01, kurtosis 3.71). The probability distribution of all the other MFs have positive and higher skewness, and much higher kurtosis. This is particularly the case for the distribution of the AF1 MF, which, having the model wind speed as denominator in the MF expression (eq. 5), evidences how the model wind is often underestimated with respect to the scatterometer wind, and results to have the longest and most populated right side tail among all the MFs, as demonstrated by its highest skewness, kurtosis and standard deviation.

To avoid unrealistic values of the mitigated wind speeds, we apply two sets of thresholds: the first filters out insufficient or excessive values of the MFs, setting each MF value outside the interval [0.9 1.2] to the nearest of the two limits: the 58% of the MF values is in this range. The second set of thresholds acts on the wind speeds, limiting too low or too high winds in input and output. The thresholds are (wind speed in ms^{-1}):

- INPUT
  - minimum scatterometer wind: 3
  - maximum scatterometer wind: 33
  - minimum number of scatterometer observations per grid point: 4
- OUTPUT
  - minimum model wind: 0
  - maximum model wind: 33

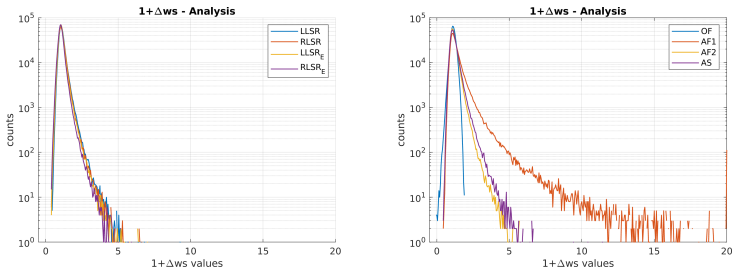

Figure 4: **Mitigation factor $(1 + \Delta w^N)$ for the forecast of dataset D3. Ordinates in log-scale.**

Model	mean	std dev	median	skewness	kurtosis
$LLSR$	1.15	0.25	1.11	3.17	36.79
$RLSR$	1.12	0.25	1.09	2.71	31.28
$LLSR_E$	1.12	0.23	1.09	3.01	34.97
$RLSR_E$	1.08	0.22	1.06	2.75	32.90
OF	1.13	0.18	1.13	-0.01	3.71
$AF1$	1.41	1.06	1.22	61.87	9531.17
$AF2$	1.19	0.27	1.14	2.61	26.16
AS	1.21	0.31	1.15	3.05	32.90

Table 1: **Summary of the statistical characteristics of the MF probability distributions. From left to right: model name, mean value, standard deviation, median value, skewness and kurtosis.**

We consider now the Taylor's diagram (Taylor, 2001) relative to the D3 dataset, which had the worst performance among the four datasets considered, as an example. The Taylor's diagram encompasses at the same time,

Preprints (www.preprints.org) | NOT PEER-REVIEWED | Posted: 28 December 2022 doi:10.20944/preprints202212.0531.v1

the values of three statistical estimators, namely the centered root mean square differences (cRMSD), the Pearson's linear correlation coefficients and the standard deviations of the original and the mitigated forecast against the scatterometer observations taken as a reference. The position of the mitigated forecast values for the eight different WBM approaches , in terms of cRMSD, linear correlation coefficient and standard deviation, are found in the Taylor's diagram of Fig. 5 (left panel), not far from the unmodified forecast. Not mitigated and mitigated forecast markers are colored according to their bias with respect to the scatterometer observations. The colorbar at the diagram's side reports the mapping between the bias color and its value. While the left panel of Fig. 5 shows the values of the four statistical indicators considering all the collocated model-scatterometer pairs, regardless of belonging to scatterometer passes in one SEV or another; the right panel reports instead the statistical indicators of the same collocated model-scatterometer pairs, but grouping by SEV all the scatterometer passes, i.e. first averaging the series (scatterometer, standard forecast, OF mitigated forecast, AF1 mitigated forecast ... etc.) within each SEV, and finally calculating the indicators (cRMSD, correlation, standard deviation and bias) on the series of the averages.

Original and mitigated forecasts have very similar statistics in terms of standard deviation, cRMSD and linear correlation: they are aligned very close in the diagram, indicating that the WBM procedure did not modify substantially the statistical properties of the model wind speed, whichever WBM algorithm is considered. However it strongly affected a fourth estimator, the wind speed bias of the mitigated forecasts, with respect to the unmodified forecasts, nudging the mitigated model fields closer to the observations with respect to the standard forecasts. While the biases remain substantially similar, wether the statistics is calculated on the series of individual pairs, or the pairs are grouped by SEV beforehands, the other three statistical indicators, namely cRMSD, correlation and standard deviation, improve when calculated on the means of the SEVs. This detail is encouraging because the effect of the wind on the surge depends on the average over large regions rather than on particular local behaviors.

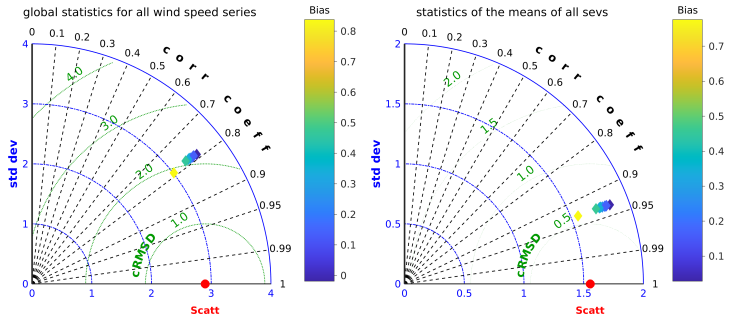

Figure 5: **Taylor's diagram showing the statistical indicators (cRMSD, linear correlation, standard deviation and bias) for the D3 dataset. Left: statistical indicators are calculated by considering all the pairs observation-model as independent. Right: the pairs observation-model are grouped by SEV and averaged, and the statistical indicators are calculated on the series of their averages.**

Table 2 (fourth row for the D3 dataset) reports the biases between the scatterometer set of observations and the corresponding set of the standard forecast in the third column, and from the fourth to the eleventh columns reports the bias between the scatterometer and the eight mitigated forecast solutions. For all the datasets the bias of the standard forecast with respect to scatterometer observations ranges from 0.84 ms^{-1}, while for the mitigated forecasts its maximum value is 0.46 ms^{-1} (minimum -0.50 ms^{-1}). In general the mitigated forecasts have lower bias, in modulus, than the standard forecast.

Dataset	# SEVs	Standard forecast	LLSR	RLSR	OF	AF1	AF2	AS	$LLSR_E$	$RLSR_E$
D1	29	0.95	0.11	0.21	0.04	-0.21	-0.01	-0.03	0.24	0.38
D2	48	0.97	0.16	0.30	0.10	-0.15	0.06	0.03	0.27	0.45
D3	364	0.84	0.24	0.34	0.19	-0.02	0.16	0.13	0.33	0.46
D4	7	0.84	-0.22	-0.08	-0.28	-0.50	-0.32	-0.35	-0.08	0.12

Table 2: **Bias of the wind speed of scatterometer and original forecast, and of scatterometer and the eight different formulation of the mitigated forecasts (in ms^{-1})**

The results for the RMSD of the mean wind speed of scatterometer and original forecast, and of scatterometer and the eight different formulation of the mitigated forecasts, grouped in SEVs, is reported in table 3. All the RMSD of the mitigated forecast winds are lower in all the eight different flavours of the mitigation, with respect to the original forecasts, for all the four datasets. It could seem that such a lower difference in the mean wind

Preprints (www.preprints.org) | NOT PEER-REVIEWED | Posted: 28 December 2022 doi:10.20944/preprints202212.0531.v1

speed values between mitigated and non-mitigated model winds has a small relevance. Actually, for storm surge modelling applications, the prominent quantity is the wind stress, which is proportional to the square of the wind speed: the relative change of the drag exerted by the wind on the sea surface is twice as large as the relative bias of the wind speed that caused it. Thus, even a small reduction of the wind speed bias between model and observations brings significant improvements, especially when the NWP data are employed to force hydrodynamic applications through the wind stress drag on the sea surface (Chelton and Freilich, 2005).

Dataset	# SEVs	Standard forecast	LLSR	RLSR	OF	AF1	AF2	AS	LLSR$_E$	RLSR$_E$
D1	29	1.00	0.60	0.63	0.60	0.67	0.61	0.61	0.61	0.68
D2	48	0.91	0.54	0.59	0.56	0.61	0.57	0.57	0.53	0.59
D3	364	0.82	0.56	0.59	0.56	0.54	0.55	0.55	0.58	0.63
D4	7	0.78	0.39	0.37	0.43	0.51	0.43	0.43	0.38	0.37

Table 3: **RMSD of the mean wind speed of scatterometer and original forecast, and of scatterometer and the eight different formulation of the mitigated forecasts, grouped in SEVs (in ms^{-1})**

Another indicator taken into consideration in the comparison is the percentage of success (POS), defined as the percentage of times that the absolute errors (AE) of the means of the mitigated winds and of the scatterometer means grouped in SEVs, resulted lower, for each dataset, than the AE of the standard forecast means and those of the observations. Table 4 reports the results of the POS for the four datsets and the eight mitigation flavours. It is worth noting that the WBM procedure is able to perform better than the forecast in a percentage of cases that ranges from 70% to 100% (mean POS: 76%). The best score is obtained by the LLSR$_E$ WBM approach, which results always the best approach for all the four datasets.

Dataset	# SEVs	LLSR	RLSR	OF	AF1	AF2	AS	LLSR$_E$	RLSR$_E$
D1	29	79	72	72	76	76	76	79	76
D2	48	79	73	73	71	75	75	81	75
D3	364	71	71	73	71	73	73	73	70
D4	7	86	71	86	57	86	86	100	86

Table 4: **Percentage of success (%)**

The numbers reported in table 4 for the D3 dataset, are derived from the data plotted in Fig. 6.

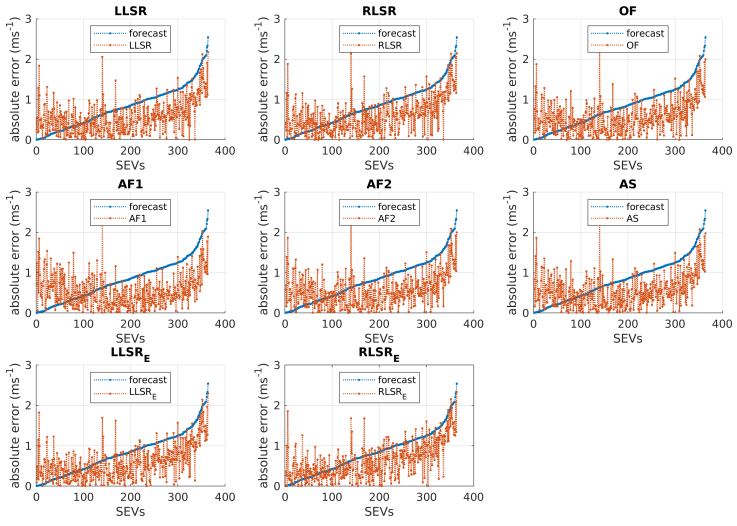

Figure 6: **Absolute error of the mean mitigated forecast and the scatterometer winds, for each SEV of dataset D3. Mitigated forecasts are marked orange, and ordered by increasing absolute error of the mean standard forecast and the scatterometer winds (in blue).**

Here, the absolute error of the mean mitigated forecast and the scatterometer winds, for each SEV of dataset D3, are plotted in orange and ordered by increasing absolute error of the mean standard forecast and the scatterometer winds. The latter are reported in blue (they are the same in all the eight plots). In practice, POS is the number of orange markers above the blue markers divided by the total number of SEVs, multiplied by one hundred. Very

Preprints (www.preprints.org) | NOT PEER-REVIEWED | Posted: 28 December 2022 doi:10.20944/preprints202212.0531.v1

little differences are seen from plot to plot, and the POS of the LLSR$_E$ MF is the same as the OF, AF2 and AS. But the LLSR$_E$ approach performs best in all four datasets, indicating the superior overall performance of this MF over the others. Another feature of the LLSE$_E$ and RLSR$_E$ MFs is that both show lower absolute errors with respect to the other MFs where the standard forecast absolute error is low (first 100 or so). On the other hand, AF1 performs better for the SEVs from 200 up to 364.

In our analysis the lower the bias and the RMSD, the better the performance. On the contrary, the POS (percentage of success) increases with the performance. In order to stick to a uniform metrics where all the indicators decrease with increasing performance, we substitute POS with the percentage of failure (POF), defined as $100 - POS$, and finally report four tables summarizing the results for the most significant statistical indicators, which are bias and POS, as the RMSD does not change significantly across the four datasets and the eight mitigation approaches, ranging between 0.51 and 0.62 ms^{-1}.

In table 5 we report RMSD, bias and POF averaged over the four datasets (by column). Table 6 does the same as table 5, but the averages are weighted by the number of cases in each dataset. The last two tables are very similar, with the exception that the dataset considered are D1, D2 and D4: the D3 dataset is omitted as it does not contain real SEVs, contrary to the other three. In each row of the four tables we have marked the two best results of the row in bold, to facilitate the verification of the mitigation factor that gave the best performance.

	LLSR	RLSR	OF	AF1	AF2	AS	LLSR$_E$	RLSR$_E$
BIAS	0.07	0.19	**0.01**	-0.22	**-0.03**	-0.05	0.19	0.35
POF	**21.25**	28.25	24.00	31.25	22.50	22.50	**16.75**	23.25

Table 5: **Bias and POF averaged over the datasets.**

	LLSR	RLSR	OF	AF1	AF2	AS	LLSR$_E$	RLSR$_E$
BIAS	0.22	0.32	0.16	**-0.05**	0.13	**0.10**	0.31	0.45
POF	27.39	28.72	26.86	28.90	**26.39**	**26.39**	**25.33**	28.83

Table 6: **Bias and POF averaged over the datasets and weighted by the number of cases in each dataset.**

	LLSR	RLSR	OF	AF1	AF2	AS	LLSR$_E$	RLSR$_E$
BIAS	**0.02**	0.14	**-0.05**	-0.29	-0.09	-0.12	0.14	0.32
POF	**18.67**	28.00	23.00	32.00	21.00	21.00	**13.33**	21.00

Table 7: **Bias and POF averaged over the datasets D1, D2 and D4, formed by real storm surge events.**

	LLSR	RLSR	OF	AF1	AF2	AS	LLSR$_E$	RLSR$_E$
BIAS	0.11	0.24	0.05	-0.20	**0.00**	**-0.02**	0.23	0.40
POF	**20.42**	27.51	26.26	28.44	23.74	23.74	**18.11**	23.74

Table 8: **Bias and POF averaged over the datasets D1, D2 and D4, and weighted by the number of cases in each dataset.**

We concentrate now on table 6 and 8: the weighted averages used to calculate the two indicators in such tables represent the truth more accurately, as the number of events varies dramatically across the four datasets. Moreover, table 6 is suitable for representing the best mitigation approach for generic situations in which real storm surge events (strong wind) alternating with weak wind events. On the contrary, table 8, considering only the three datasets formed by real storm surge events, evidences the mitigation approach most needed in case of strong winds.

In the first case (balanced occurrence of strong and weak wind), the mitigation approach that perform better are AS, followed by AF1, AF2 and LLSR$_E$; in the second (strong wind and thus optimized for storm surges), four approaches perform equally well: LLSR, AF2, AS and LLSR$_E$. Thus, AS resulted the best performing and versatile mitigation approach, followed by AF2 and LLSR$_E$.

SUMMARY AND CONCLUSIONS

In this study we have analyzed the structural and statistical aspects of a numerical method developed to reduce the bias between the sea surface wind observed by the scatterometers and that forecasted by a numerical model.

Preprints (www.preprints.org) | NOT PEER-REVIEWED | Posted: 28 December 2022 doi:10.20944/preprints202212.0531.v1

The method is called "bias mitigation", and relies on scatterometer observations to determine a correction factor $(1 + \Delta w^N)$ to modulate the standard model wind as: $w'^{model} = w^{model}(1 + \Delta w^N)$. We compared eight different mathematical formulations of deriving the factor Δw^N, namely:

- three linear-like: LLSR, AS, LLSR$_E$;
- five relative-like: RLSR, OF, AF1, AF2, RLSR$_E$.

We have derived some statistical parameters for the eight mitigation approaches, using four datasets:

- Dataset D1: 29 SEVs (observed surge in Venice ¿40 cm) during the years 2004–2014;
- Dataset D2: 48 SEVs (observed surge in Venice ¿40 cm) during the years 2013–2016;
- Dataset D3: 364 random wind cases during the years 2013–2016;
- Dataset D4: 7 SEVs in 2012–2016 for which the local tide forecasting authority of Venice predicted the high water worse.

We found that the standard forecast and the eight mitigated forecasts have similar centered RMSD $(scatt - model)$, comparable Pearson's linear correlation coefficient and similar standard deviation. But, most important, the mitigated forecasts have in general a significantly smoller bias, with respect the scatterometer observations, than the standard forecast.

The analyses have demonstrated that the RMSD $(scatt - model)$ of the eight mitigated forecasts are almost constant across the four datasets and the eight methods, evidencing its low sensitivity. For this reason, the following conclusions are based only on the other two indicators considered: the bias and the percentage of failure/success. The bias of the eight mitigated forecasts ranged between -0.50 and 0.46 ms^{-1}, and are always low compared to the standard forecast, which is always lower that the scatterometer observations by 0.85 to 0.97 ms^{-1}.

The mitigated forecasts also performed better than the standard forecast in more than 70 % of the cases. The POS has been shown to remain high (¿ 70 %) across the four different datasets and the eight mathematical formulations of the mitigation factor, demonstrating the possibility of improving the model forecast wind speed using scatterometer observations, in a operational-like configuration, through the WBM technique. A more accurate wind speed determines a better prediction of the surge levels: in the Gulf of Venice and the Venice Lagoon it is of the utmost importance to rely on good forcing fields for the correct prediction of the high waters, even now that the MO.SE. barriers have been put into operation.

Among the eight formulations considered for the wind bias mitigation, the most performant and balanced resulted AS, followed close by LLSR$_E$ and AF2. The other formulations (OF, AF1, LLSR, RLSR, RLSR$_E$) performed slightly worse, but are still closer to scatterometer observations than the standard model forecast.

The bias mitigation procedure appears to bring advantages both when the meteorological conditions are favourable to storm surge and when the meteorological configuration are random, but in this last case it is slightly less efficient. The mitigation procedure can be adopted in operational context, as it uses scatterometer observation (∼3h latency), ECMWF model analysis fileds (∼7h latency) and ECMWF model forecast fields (∼7h latency). There is still the need to investigate about wind direction bias, to analyze the performance in other regions and to assess the possible causes that determine the failure of the method in almost the 25% of the cases.

ACKNOWLEDGMENTS

The QuikSCAT and Oceansat-2 winds have been processed by the Jet Propulsion Laboratory/California Institute of Technology; the ASCAT winds by the EUMETSAT Ocean and Sea Ice Satellite Application Facility (OSI-SAF). The satellite winds have been downloaded from the NASA Physical Oceanography Distributed Active Archive Center (PO.DAAC) at the Jet Propulsion Laboratory/California Institute of Technology. The ECMWF fields have been obtained thanks to the authorization from the Aereonautica Militare Italiana. This work has been supported by the project Storm Surge for Venice (eSurge-Venice, `http://www.esurge-venice.eu`) funded by the European Space Agency as part of its Data User Element (DUE) programme, as well as by the Flagship Project RITMARE (`http://www.ritmare.it`) funded by the Italian Ministry of University and Research. The study has been conducted in the framework of the *Technical and Scientific Collaboration Agreement* between the *Institute of Atmospheric Sciences and Climate* of the *National Research Council of Italy* and the *Tide Forecast and Early Warning Centre* of the *Venice Municipality*.

 doi:10.20944/preprints202212.0531.v1

References

Accadia, C., Zecchetto, S., Lavagnini, A., and Speranza, A. (2007). Comparison of 10-m Wind Forecasts from a Regional Area Model and QuikSCAT Scatterometer Wind Observations over the Mediterranean Sea. *Mon. Wea. Rev.*, 135:1945–1960.

Bajo, M., De Biasio, F., Umgiesser, G., Vignudelli, S., and Zecchetto, S. (2017). Impact of using scatterometer and altimeter data on storm surge forecasting. *Ocean Modelling*, 113(Supplement C):85–94.

Byrne, D., Horsburgh, K., Zachry, B., and Cipollini, P. (2017). Using remotely sensed data to modify wind forcing in operational storm surge forecasting. *Natural Hazards*, 89(1):275–293.

Chelton, D. and Freilich, M. (2005). Scatterometer-based assessment of 10-m wind analyses from the operational ECMWF and NCEP numerical weather prediction models. *J. of Geophys. Res.*, 133:409–429.

Church, J. A., Clark, P. U., Cazenave, A., Gregory, J. M., Jevrejeva, S., Levermann, A., Merrifield, M. A., Milne, G. A., Nerem, R. S., Nunn, P. D., Payne, A. J., Pfeffer, W. T., Stammer, D., and Unnikrishnan, A. S. (2013). Sea Level Change. In Stocker, T. F., Qin, D., Plattner, G. K., Tignor, M., Allen, S. K., Boschung, J., Nauels, A., Xia, Y., Bex, V., and Midgley, P. M., editors, *Climate Change 2013: The Physical Science Basis. Contribution of Working Group I to the Fifth Assessment Report of the Intergovernmental Panel on Climate Change*, chapter 13, pages 1137–1216. Cambridge University Press, Cambridge, United Kingdom and New York, NY, USA.

De Biasio, F., Bajo, M., Vignudelli, S., Umgiesser, G., and Zecchetto, S. (2017). Improvements of storm surge forecasting in the Gulf of Venice exploiting the potential of satellite data: the ESA DUE eSurge-Venice project. *European Journal of Remote Sensing*, 50:428–441.

De Biasio, F., Vignudelli, S., della Valle, A., Umgiesser, G., Bajo, M., and Zecchetto, S. (2016). Exploiting the potential of satellite microwave remote sensing to hindcast the storm surge in the Gulf of Venice. *IEEE Journal of Selected Topics in Applied Earth Observations and Remote Sensing*, 9:5089–5105.

JPL (2013a). Oceansat-2 Level 2B User Guide. Guide document, version 1.0, Jet Propulsion Laboratory, Pasadena, USA.

JPL (2013b). QuikSCAT Level 2B Version 3. Guide document, version 1.0, Jet Propulsion Laboratory, Pasadena, USA.

Kara, A. B., Wallcraft, A. J., Martin, P. J., and Pauley, R. L. (2009). Optimizing surface winds using QuikSCAT measurements in the Mediterranean Sea during 2000–2006. *Journal of Marine Systems*, 78(Supplement):119–131.

Lionello, P., Cavaleri, L., Nissen, K., Pino, C., Raicich, F., and Ulbrich, U. (2012). Severe marine storms in the Northern Adriatic: Characteristics and trends. *Physics and Chemistry of the Earth, Parts A/B/C*, 40–41:93–105. The Climate of Venetia and Northern Adriatic.

OSISAF (2012). ASCAT Wind Product User Manual. Version 1.22. Technical Report SAF/OSI/CDOP/KNMI/TEC/MA/126, Eumetsat, Darmstadt, Germany.

Pugh, D. T. (1987). *Tides, Surges and Mean Sea Level: A Handbook for Engineers and Scientists*. John Wiley and Sons, Chichester, UK.

Silvester, R. (1971). Computation of storm surge. In *Proceedings of the 12th Conference on Coastal Engineering*, pages 1995–2010.

Stark, J., Donlon, C., Martin, M., and McCulloch, M. (2007). OSTIA : An operational, high resolution, real time, global sea surface temperature analysis system. In *OCEANS 2007 - Europe*, pages 1–4.

Taylor, K. E. (2001). Summarizing multiple aspects of model performance in a single diagram. *Journal of Geophysical Research-A*, 106:7183–7192.

Tofallis, C. (2008). Least Squares Percentage Regression. *Journal of Modern Applied Statistical Methods*, 7(2):526–534.

 doi:10.20944/preprints202212.0531.v1

W.T. Liu and K.B. Katsaros and J.A. Businger (1979). Bulk parameterization of air–sea exchange of heat and water vapor including the molecular constraints at the interface. *J. Atmos. Sci.*, 36:1722–1735.

Zecchetto, S., De Biasio, F., and Accadia, C. (2013). Scatterometer and ECMWF-derived wind vorticity over the Mediterranean Basin. *Quarterly Journal of the Royal Meteorological Society*, 139(672):674–684.

Zecchetto, S., della Valle, A., and De Biasio, F. (2015). Mitigation of ECMWF–scatterometer wind biases in view of storm surge applications in the Adriatic Sea. *Advances in Space Research*, 55(5):1291–1299.

Zecchetto, S. and Accadia, C. (2014). Diagnostics of T1279 ECMWF analysis winds in the Mediterranean basin by comparison with ASCAT 12.5 km winds. *Quarterly Journal of the Royal Meteorological Society*, 140(685):2506–2514.